



Communication

Reduction of mercury(II) by electrons contained in carbon dots: An environmentally friendly cold vapor generation for mercury analysis

Tao Chen^a, Yao Lin^a, Haochen Li^b, Rui Yang^a, Xiandeng Hou^{a,c}, Baozhan Zheng^{a,*}, Chengbin Zheng^{a,*}^a Key Laboratory of Green Chemistry and Technology, Ministry of Education, College of Chemistry, Sichuan University, Chengdu 610064, China^b Chengdu No. 7 High School, Chengdu 610041, China^c Analytical & Testing Center, Sichuan University, Chengdu 610064, China

ARTICLE INFO

Article history:

Received 28 March 2020

Received in revised form 20 May 2020

Accepted 2 June 2020

Available online 3 June 2020

Keywords:

Mercury analysis

Reduction

Carbon dots

Cold vapor generation

ABSTRACT

In this work, the reduction of mercury ions (Hg^{2+}) to elemental mercury (Hg^0) was easily achieved using highly reductive carbon dots (r-CDs), which synthesized from sucrose by a simple and cost-effective method. After a careful mechanistic study, the reduction was probably accomplished with the large numbers of electrons contained in r-CDs rather than the oxidation of its functional groups. Additionally, a 3-(4,5-dimethylthiazol-2-yl)-2,5-diphenyltetrazolium bromide (MTT) assay showed that the r-CDs were nontoxic to wildlife and human beings. Consequently, the r-CDs were used as an alternative to toxic reductants (SnCl_2 or NaBH_4) for the sensitive and *in situ* determination of mercury by cold vapor generation (CVG) coupled to a miniature point discharge optical emission spectrometer ($\mu\text{PD-OES}$). Limit of detection of $0.05 \mu\text{g/L}$ was obtained for Hg^{2+} , with relative standard deviation (RSD) less than 5.4% at a concentration of $5 \mu\text{g/L}$. The accuracy of r-CDs induced CVG- $\mu\text{PD-OES}$ was validated by the determination of mercury in a certified reference material (DOLT-5, dogfish liver) and five natural water samples collected from different rivers and lakes in Chengdu City. Since r-CDs are nontoxic and prepared from abundant and inexpensive sucrose, the r-CDs induced CVG- $\mu\text{PD-OES}$ retains the great potential for the inexpensive and environmentally friendly field analysis of mercury in natural water. The accuracy of the proposed method was validated by the analysis of a certified reference material and several water samples with satisfactory results.

© 2020 Chinese Chemical Society and Institute of Materia Medica, Chinese Academy of Medical Sciences.

Published by Elsevier B.V. All rights reserved.

Mercury (Hg) is regarded as the most ubiquitous pollutant in the environment. It has drawn global attention because of its properties of persistence, toxicity, long-range transport, and bioaccumulation in the environment. Exposure to Hg, even at extreme low doses, can cause severe effects on human and wildlife health [1–4]. As part of the United Nations Environment Programme (UNEP), the governments from 140 countries signed the Minamata Convention on mercury to decrease the mercury emission from the anthropogenic activities, demonstrating the global urgency of detection of this persistent toxin [5].

Although mercury analysis can be easily realized using commercial atomic spectrometry, the conventional commercial atomic spectrometers (atomic absorption (AAS), atomic fluorescence (AFS) and inductively coupled plasma optical emission/mass

spectrometers (ICP-OES/ICP-MS)) are too bulky, expensive, heavy, and energy consuming, which can only be operated in the laboratory [6,7]. To cope with accidents caused by either unexpected leakage or illegal disposal of mercury-containing substances, it requires environmental monitoring using portable atomic spectrometer for quick and *in situ* monitoring of mercury [8]. Recently, microplasma atomic spectrometers have been found to retain the promising potential for field analysis of toxic metals owing to their unique advantages of simple experimental setup, low-energy, and minimal gas consumption [9–12]. Unfortunately, the power of the microplasma is only a dozen watts and a majority of the energy is wasted on sample evaporation and desolvation. Therefore, their sensitivities are too low to be used for the direct analysis of mercury in environmental samples. Thus, significant effort has been dedicated to developing an efficient sampling technique to improve the performance of microplasma atomic spectrometry. Cold vapor generation (CVG) is a mature and prevailing sample introduction method, which can efficiently separate Hg^0 from the liquid phase before introduction to the

* Corresponding authors.

E-mail addresses: zhengbaozhan@scu.edu.cn (B. Zheng), abinscu@scu.edu.cn (C. Zheng).

atomic spectrometer, thus eliminating the power wasted on sample evaporation and desolvation, improving the introduction efficiency of analyte and sensitivity [13–15]. However, there are some disadvantages associated with conventional CVG using $\text{NaBH}_4\text{-HCl}$ or $\text{SnCl}_2\text{-HCl}$ system, which need to be overcome before their application to field analysis of mercury [16–18]. Firstly, the generation of secondary pollution during field analysis using the toxic chemicals. Secondly, $\text{NaBH}_4\text{-HCl}$ produces a large amount of hydrogen, which significantly depresses or even extinguishes microplasma. Recently, photochemical vapor generation (PVG) [19–22], ultrasound-promoted CVG [23], microplasma induced CVG [24–26] have been developed to resolve these problems to some extent.

Over the past two decades, carbon dots (CDs) have attracted considerable attention and intensively used for bioimaging, photocatalysis, and optoelectronic sensors due to their unique optical properties, good biocompatibility, high photostability, and low toxicity [27–30]. Although the electron transfer between CDs and metal ions has been widely utilized for the determination of toxic metals ions (including Hg^{2+}) via induced turn-on/turn-off fluorescence [31–33], the reduction of Hg^{2+} to Hg^0 through the electron transfer has never been found.

Herein, highly hydrophilic reductive carbon dots (r-CDs) were synthesized from sucrose by a simple and cost-effective method (Scheme 1a). The synthesized r-CDs not only possess excellent fluorescence properties but also show distinct reduction potential to convert Hg^{2+} to Hg^0 , thus serving as an alternative to SnCl_2 or NaBH_4 to achieve CVG of Hg^{2+} . Consequently, combined with miniaturized battery-powered point discharge optical emission spectrometry ($\mu\text{PD-OES}$), the r-CDs induced cold vapor generation (r-CDI-CVG) with headspace sample introduction was utilized for the field analysis of mercury, as shown in Scheme 1b. The schemes of $\mu\text{PD-OES}$ was illustrated in Fig. S1 (Supporting information).

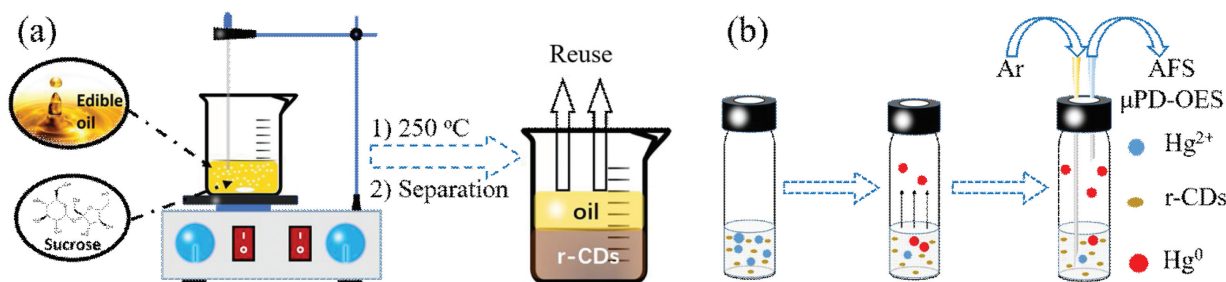
The morphology and size of r-CDs were characterized by transmission electron microscopy (TEM). As shown in Fig. 1a, the synthesized r-CDs are monodispersed spherical nanoparticles with an average size of 3.15 ± 0.41 nm (inset of Fig. 1a). From the high-resolution transmission electron microscopy (HRTEM) image (Fig. 1b), a portion of the particles with well-resolved lattice fringes can be observed, demonstrating the presence of well-crystallized structure in the synthesized r-CDs. The lattice spacing is about 0.20 nm (inset of Fig. 1b), which is consistent with that of the in-plane lattice spacing of graphene (100 facets) [34]. The X-ray diffraction (XRD) pattern of the r-CDs presented in Fig. 1c, shows no apparent peaks, other than a broad diffraction peak at 22° , indicating the co-existence of disordered carbon structure in the synthesized r-CD [35], which is consistent with the morphology results from TEM. To investigate the composition of the r-CDs and its functional groups on the surface, the Fourier transform infrared (FTIR) spectrum of r-CDs was also recorded and shown in Fig. 1d. The broad absorption peak at $3100\text{--}3600\text{ cm}^{-1}$ is attributed to the stretching vibrations of O—H, which implies the presence of abundant hydroxyl groups on the prepared r-CDs, resulting the

excellent dispersibility of r-CDs in aqueous solution [36]. The sharp peak at 1049 cm^{-1} was assigned to the stretching vibration of C—O [37], and the peak at 1643 cm^{-1} could be the stretching vibration of C=C, which resulted from the dehydration of sucrose during the synthesis procedure [36]. Moreover, the peak at 1726 cm^{-1} belongs to the stretching vibration of C=O owing to the oxidation of —OH groups [38]. The surface structure of r-CDs was further investigated by X-ray photoelectron spectroscopy (XPS), as shown in Fig. 1e. The r-CDs were mainly composed of carbon and oxygen according to the typical peaks of C 1s (285.4 eV) and O 1s (532.6 eV). The C 1s spectrum (Fig. 1f) can be divided into three surface components, corresponding to the C—C/C=C (284.5 eV), C—O (286.1 eV) and C=O (288.5 eV), [39] respectively, which was consistent with results from FTIR.

The optical properties of r-CDs were also investigated via UV–vis absorption and fluorescence (Fig. S2 in Supporting information). Two absorption peaks at 282 nm and 226 nm can be observed, relating to the $n\text{-}\pi^*$ transition and $\pi\text{-}\pi^*$ in r-CDs [40], respectively. The maximum fluorescence emission wavelengths of r-CDs are centered at 445 nm with an excitation at 355 nm, indicating the formation of CDs [35]. Additionally, a 3-(4,5-dimethylthiazol-2-yl)-2,5-diphenyltetrazolium bromide (MTT) assay was undertaken (Fig. S3 in Supporting information) and it can be observed that the viability of HeLa cells exceeds 96% even after incubation with 1 mg/mL of r-CDs for 24 h, which demonstrates the synthesis of r-CDs by this oil-bath method exhibits very low cytotoxicity.

As a highly efficient sampling method, CVG has been widely used in atomic spectrometry with the advantages of less matrix interference and high transport efficiency [19–26]. So far, there has been no report of the use of CDs as a reductant to induce CVG. An initial experiment was undertaken to verify the feasibility of r-CDI-CVG. A 1 mL sample volume of standard solution containing 20 $\mu\text{g/L}$ Hg^{2+} together with r-CDs was placed in a brown vial. After mixing and reaction, 400 mL/min of Ar was used to sweep the generated volatile Hg^0 into the AFS for detection. The atomic fluorescence signal obtained is presented in Fig. 2a. With the addition of 20 $\mu\text{g/L}$ Hg^{2+} ions, a remarkable 10-fold enhancement of response can be achieved in the presence of 5 mg/mL r-CDs, demonstrating the strong reducing capability of r-CDs for the reduction of Hg^{2+} to volatile Hg^0 . Further, r-CDI-CVG was also coupled with $\mu\text{PD-OES}$ to evaluate its practicability for field analysis of environmental samples for Hg^{2+} . A blank and a standard solution containing 100 $\mu\text{g/L}$ Hg^{2+} were detected by r-CDI-CVG- $\mu\text{PD-OES}$, and results are summarized in Fig. 2b. Typical molecular emission bands from OH (283, 309, 319 nm), NH (337 nm) and N_2 (358, 380 nm) were found in both spectra, which is consistent with previous work [41]. Obviously, the atomic emission bands for Hg (253.65 nm and 365.01 nm) can be distinguished from that of the background, which demonstrates the feasibility of this method for the field analysis of mercury (Fig. 2c).

The experimental parameters affecting the efficiency of r-CDI-CVG and $\mu\text{PD-OES}$ were further investigated (Figs. S4 and S5 in



Scheme 1. (a) Synthesis of r-CDs via the oil-bath method. (b) The generation and analysis process of volatile Hg^0 .

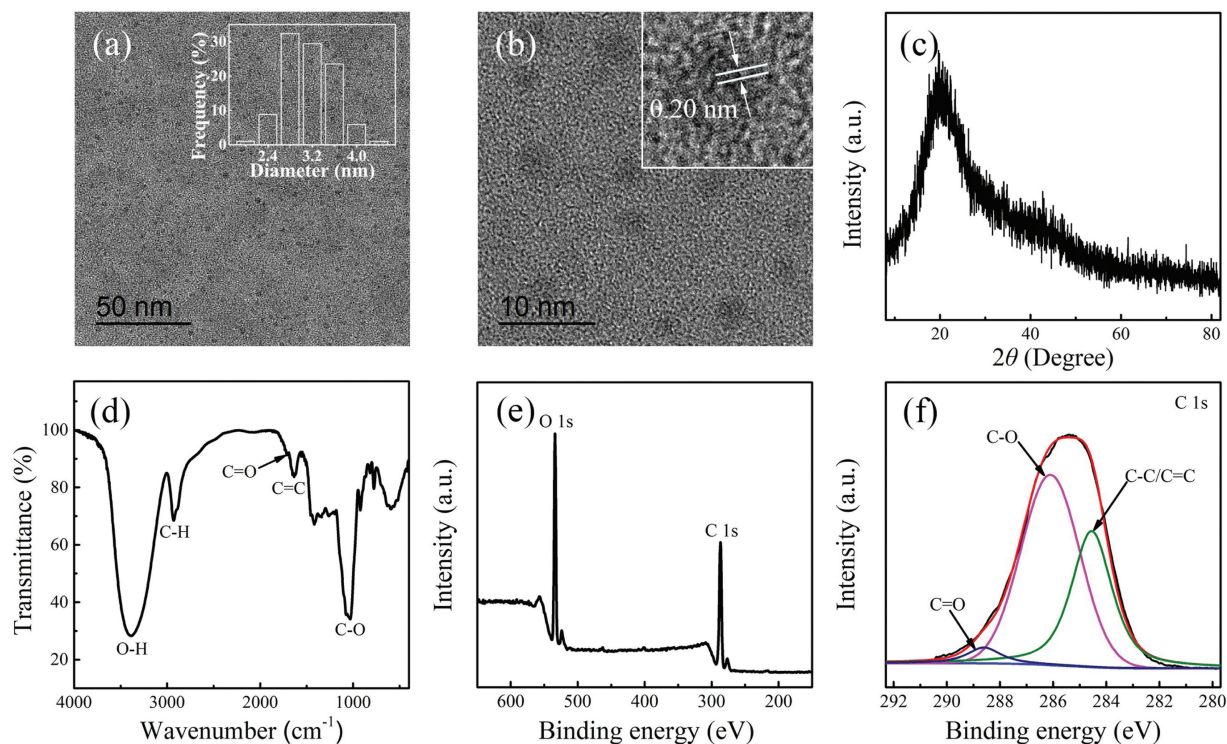


Fig. 1. (a) TEM image and size distribution of r-CDs (inserted image). (b) HRTEM image of r-CDs. (c) XRD pattern of the synthesized r-CDs. (d) FTIR spectra of r-CDs. (e) XPS spectrum of r-CDs and (f) high-resolution spectra of the C 1s.

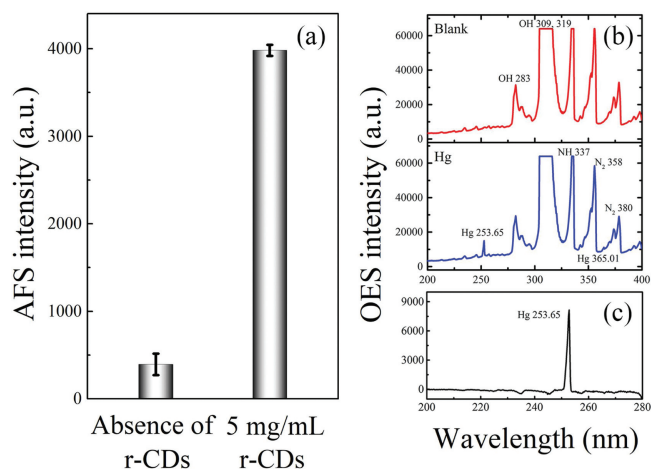


Fig. 2. (a) Atomic fluorescence intensity from r-CDI-CVG-AFS with 20 $\mu\text{g/L}$ Hg^{2+} in the absence/presence of r-CDs. (b) Emission spectra generated by r-CDI-CVG- $\mu\text{PD-OES}$ without/with Hg^{2+} , and (c) mercury emission spectra after calibration.

Supporting information). Under optimal experimental conditions, the analytical performance of r-CDI-CVG-AFS/ $\mu\text{PD-OES}$ was evaluated. The OES signal profiles of Hg shown in Fig. 3a indicate that the Hg emission intensity gradually increases with the increase concentration of Hg^{2+} . Calibration curves were obtained and shown in Fig. 3b, showing linear coefficients (R^2) better than 0.99, along with the achieved ranges of 0.5–100 $\mu\text{g/L}$. The Hg^{2+} -dependent calibration curve was also obtained by AFS, as shown in Fig. S6 (Supporting information). The limit of detection (LOD), defined as the analyte concentration calculated by using the three-fold standard deviation of 11 measurements of a blank solution divided by the slope of the calibration curve, were 0.002 $\mu\text{g/L}$ and 0.05 $\mu\text{g/L}$ for mercury by AFS and $\mu\text{PD-OES}$. The precision, expressed as the relative standard deviation (RSD, $n = 11$)

obtained by both AFS and $\mu\text{PD-OES}$ are less than 5.4% (Fig. 3c). Table S1 (Supporting information) summarizes the figures of merit achieved with the methodology compared with other conventional methods. It can be concluded that the proposed method not only retains a comparable or even better LOD than those obtained by other CVG techniques for the analysis of mercury, but they also provide several unique advantages, including portability, less power consumption, and greener analytical methodology.

One serious problem with the conventional methods based on flow injection or continuous sample introduction for the determination of mercury is the memory effect, particularly at ultra-trace levels. To demonstrate the free memory effect for headspace sample introduction with the r-CDI-CVG, a series of mercury standard solutions were analyzed by the proposed method from high to low concentration. From the results shown in Fig. S7 (Supporting information), the linear correlation coefficient is still better than 0.99, therefore, any memory effect occurring with the proposed method is negligible. The CVG efficiency was estimated via a comparison of the Hg^{2+} concentrations in the solutions before and after the reaction. The results summarized in Fig. S8 (Supporting information) show that $72\% \pm 2\%$ of vapor generation efficiency is obtained, suggesting the efficient reduction of Hg^{2+} using the synthesized r-CDs as reductant.

A CRM and several water samples were used to validate the accuracy and practicality of the routine analysis of mercury by r-CDI-CVG-AFS/ $\mu\text{PD-OES}$, the results summarized in Table S2 (Supporting information). The recoveries calculated from spiking standard into the real samples were in range of 85%–113%. A t -test showed that the analytical results obtained by the method are not different from the certified values at 95% level of confidence. Furthermore, the HG-AFS method was taken to compare with r-CDI-CVG-AFS, as shown in Table S3 (Supporting information), 0.5 $\mu\text{g/L}$ of mercury were added into water samples, both AFS methods shows satisfactory recoveries and consistent results.

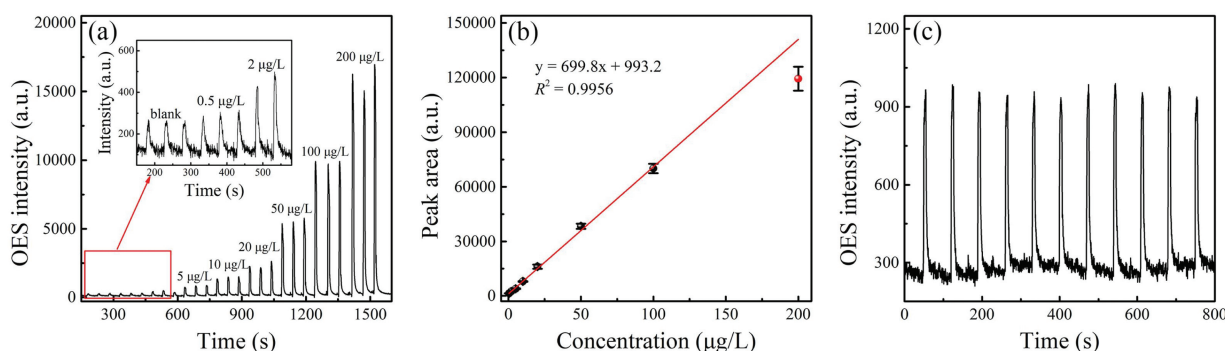


Fig. 3. (a) Hg emission signal profiles of r-CDI-CVG- μ PD-OES. (b) Calibration curves established using r-CDI-CVG- μ PD-OES. (c) Hg emission signal profiles of 11 replicate measurements of 5 μ g/L Hg^{2+} ions.

To gain insight into the r-CDI-CVG, the possible mechanism for the reduction of Hg^{2+} by r-CDs was investigated. According to the results from FTIR, the prepared r-CDs have large amounts of hydroxyl groups on their surfaces which allow for not only good hydrophilicity for uniform dispersion of the r-CDs but also excellent reducibility in water. It has been reported that Au^{3+} is reduced to gold nanoparticles by the hydroxyl groups on the surface of carbon dots [42]. Thus, Hg^{2+} can be considered to be reduced by the hydroxyl groups of r-CDs. To support this view, excessive Hg^{2+} was added to the solution of r-CDs. After reaction for 40 min, the r-CDs were collected and characterized by attenuated total reflection infrared (ATR-IR) and UV-vis absorption spectrometry. Unexpectedly, there is no obvious new characteristic peak or band shift observed in both ATR-IR and UV-vis spectra (Figs. S9a and S10 in Supporting information), which demonstrates that there is no generation of a new functional group after the reduction of Hg^{2+} , indicating that the hydroxyl groups on the surface of r-CDs are not altered by Hg^{2+} .

It has been demonstrated that CDs with large amounts of hydroxyl groups usually contain many electrons. Thus, Hg^{2+} is likely reduced by the electrons rather than the hydroxyl groups. To verify this speculation, the effect of Hg^{2+} on the fluorescence of r-CDs was carefully investigated. The analytical results (Fig. S11a in Supporting information) show that the fluorescence intensity decreased with the increasing concentration of Hg^{2+} , which may be because Hg^{2+} consumed the electrons and weakened the conjugated effect of the $n-\pi$ system. Another experiment was undertaken to further support this speculation. 10 mg/L of Fe^{3+} was added to the r-CDs solution prior to the addition of Hg^{2+} and the generation efficiency of Hg^0 was found to be significantly depressed to as low as 10%. To gain insight into the reaction between r-CDs and Fe^{3+} , the product of Fe^{3+} after the reaction was first tested using a potassium ferricyanide solution, as shown in Fig. S12 (Supporting information). Cyan precipitation appears in the mixture of Fe^{3+} and r-CDs after the addition of potassium ferricyanide, whereas no change was found in the solution

containing Fe^{3+} or r-CDs alone, which implies that the product of Fe^{3+} is Fe^{2+} . Moreover, the r-CDs obtained before and after the reaction with Fe^{3+} were also characterized by ATR-IR spectrometry, UV-vis and fluorescence spectrometry. Both ATR-IR (Fig. S9b in Supporting information) and UV-vis (Fig. S10 in Supporting information) spectra show that the functional groups on the r-CDs have not been altered during reaction. The fluorescence intensity of r-CDs (Fig. S11b in Supporting information) also gradually decreased with increasing concentration of Fe^{3+} , which is similar to the results obtained after the addition of Hg^{2+} . Together, these results indicate that Fe^{3+} consumes large amounts of electrons, resulting in inefficient reduction of Hg^{2+} . Based on all the aforementioned observations, we conclude that Hg^{2+} is most likely reduced by the electrons contained in the r-CDs, and the possible process is illustrated in Fig. 4. Hg^{2+} consumes large amounts of electrons inside r-CDs, resulting in the reduction of Hg^{2+} to Hg^0 . The interferences from other potential co-existing on the r-CDI-CVG of mercury were also investigated (Table S4 in Supporting information) and it is evident that no obvious interferences from the tested ions.

Highly r-CDs have been easily synthesized using inexpensive and readily available sucrose as the raw material, which possess excellent capability for the reduction of Hg^{2+} to Hg^0 . Based on a careful mechanistic study, Hg^{2+} is probably reduced by the electrons contained in r-CDs instead of hydroxyl groups on the surface. Owing to its distinguished reducibility, the synthesized r-CDs were used as a cost-effective and environmentally friendly reductant for the reduction of Hg^{2+} . Therefore, the r-CDI-CVG has been successfully coupled to a laboratory-constructed battery-powered μ PD-OES for the highly sensitive detection of trace mercury. Due to the many advantages arising from both the prepared r-CDs and the battery-powered μ PD-OES, including low cost, environmental friendliness, small footprint, simple operation, as well as low gas and power consumption, the r-CDI-CVG- μ PD-OES presents promising potential for the field analysis of mercury. Meanwhile, since it is nontoxic and prepared from

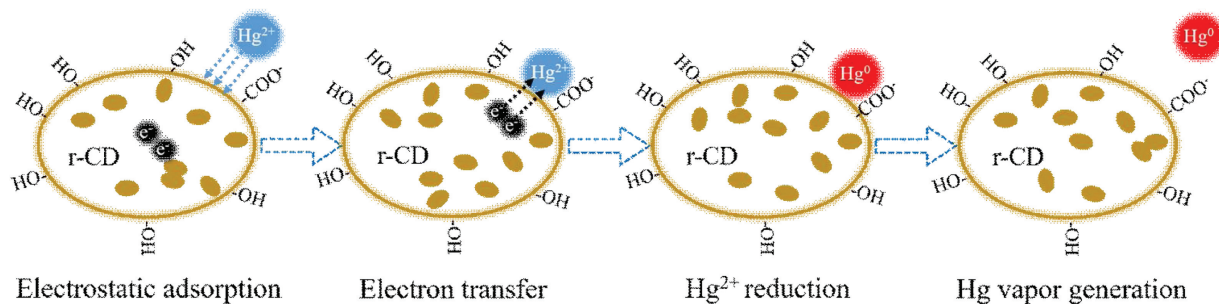


Fig. 4. The possible process of the reduction of mercury ions.

abundant and inexpensive sucrose, the r-CDs also retains the great potential for the inexpensive, rapid and environmentally friendly removal of mercury from contaminated water.

Declaration of competing interest

The authors declare that there are no conflicts of interest.

Acknowledgments

We would like to thank Prof. Li Wu and Prof. Yunfei Tian (Analytical and Testing Center, Sichuan University) for their technical assistance. The authors gratefully acknowledge the National Natural Science Foundation of China (Nos. 21529501, 21622508 and 21575092) for financial support. H. Li appreciates the financial support from the high school talent plan of China Association for Science and Technology.

Appendix A. Supplementary data

Supplementary material related to this article can be found, in the online version, at doi:<https://doi.org/10.1016/j.ccllet.2020.06.005>.

References

- [1] H.H. Harris, I.J. Pickering, G.N. George, *Science* 301 (2003) 1203.
- [2] P.B. Tchounwou, W.K. Ayensu, N. Ninashvili, et al., *Environ. Toxicol.* 18 (2003) 149–175.
- [3] X.R. Hu, Y.X. Zhang, *Chin. Chem. Lett.* 15 (2004) 326–329.
- [4] E.M. Nolan, S.J. Lippard, *Chem. Rev.* 108 (2008) 3443–3480.
- [5] J. Qiu, *Nature* 493 (2013) 144–145.
- [6] J.R. Bacon, O.T. Butler, W.R. Cairns, et al., *J. Anal. At. Spectrom.* 34 (2019) 9–58.
- [7] D. Pröfrock, A. Prange, *Appl. Spectrosc.* 66 (2012) 843–868.
- [8] N. Idros, D. Chu, *ACS Sens.* 3 (2018) 1756–1764.
- [9] B. Han, X. Jiang, X. Hou, et al., *Anal. Chem.* 86 (2014) 6214–6219.
- [10] Y. Lin, Y. Yang, Y. Li, et al., *Environ. Sci. Technol.* 50 (2016) 2468–2476.
- [11] S. Zhang, Y. Tian, H. Yin, et al., *Environ. Sci. Technol.* 51 (2017) 9109–9117.
- [12] C. Cheng, L. Hu, X. Hou, et al., *Anal. Chem.* 90 (2018) 3683–3691.
- [13] R.E. Sturgeon, Z. Mester, *Appl. Spectrosc.* 56 (2002) 202A–213A.
- [14] P. Wu, L. He, C. Zheng, et al., *J. Anal. At. Spectrom.* 25 (2010) 1217–1246.
- [15] Z. Li, Q. Tan, X. Hou, et al., *Anal. Chem.* 86 (2014) 12093–12099.
- [16] Z. Zhu, G.C. Chan, S.J. Ray, et al., *Anal. Chem.* 80 (2008) 8622–8627.
- [17] V. Cervený, M. Horváth, J.A.C. Broekaert, *Microchem. J.* 107 (2013) 10–16.
- [18] A. Leng, Y. Tian, M. Wang, et al., *Chin. Chem. Lett.* 28 (2017) 189–196.
- [19] C. Zheng, L. Yang, R.E. Sturgeon, et al., *Anal. Chem.* 82 (2010) 3899–3904.
- [20] S. Zhang, H. Luo, M. Peng, et al., *Anal. Chem.* 87 (2015) 10712–10718.
- [21] C. Zheng, R.E. Sturgeon, C. Brophy, et al., *Anal. Chem.* 82 (2010) 3086–3093.
- [22] C. Zheng, Y. Li, Y. He, et al., *J. Anal. At. Spectrom.* 20 (2005) 746–750.
- [23] S. Gil, I. Lavilla, C. Bendicho, et al., *Anal. Chem.* 78 (2006) 6260–6264.
- [24] Z. Zhu, G.C. Chan, S.J. Ray, et al., *Anal. Chem.* 80 (2008) 7043–7050.
- [25] Q. Chen, Y. Lin, Y. Tian, et al., *Anal. Chem.* 89 (2017) 2093–2100.
- [26] S. Xia, A. Leng, Y. Lin, et al., *Anal. Chem.* 91 (2019) 2701–2709.
- [27] W. Lv, X. Wang, J. Wu, et al., *Chin. Chem. Lett.* 30 (2019) 1635–1638.
- [28] S. Cui, Y. Wu, Y. Liu, et al., *Chin. Chem. Lett.* 31 (2020) 487–493.
- [29] H. Wang, J. Wei, C. Zhang, et al., *Chin. Chem. Lett.* 31 (2020) 759–763.
- [30] J. Zhong, X. Chen, M. Zhang, et al., *Chin. Chem. Lett.* 31 (2020) 769–773.
- [31] I. Costas-Mora, V. Romero, I. Lavilla, et al., *Anal. Chem.* 86 (2014) 4536–4543.
- [32] H. Lu, S. Xu, J. Liu, *ACS Sens.* 4 (2019) 1917–1924.
- [33] W. Li, Y. Liu, B. Wang, et al., *Chin. Chem. Lett.* 30 (2019) 2323–2327.
- [34] Y. Dong, H. Pang, H.B. Yang, et al., *Angew. Chem. Int. Ed.* 52 (2013) 7800–7804.
- [35] S. Zhu, Q. Meng, L. Wang, et al., *Angew. Chem. Int. Ed.* 52 (2013) 3953–3957.
- [36] Z.C. Yang, M. Wang, A.M. Yong, et al., *Chem. Commun.* 47 (2011) 11615–11617.
- [37] Z.L. Wu, P. Zhang, M.X. Gao, et al., *J. Mater. Chem. B Mater. Biol. Med.* 1 (2013) 2868–2873.
- [38] L. Shen, M. Chen, L. Hu, et al., *Langmuir* 29 (2013) 16135–16140.
- [39] L. Tang, R. Ji, X. Cao, et al., *ACS Nano* 6 (2012) 5102–5110.
- [40] Z. Luo, Y. Lu, L. Somers, et al., *J. Am. Chem. Soc.* 131 (2009) 898–899.
- [41] Y. Yang, Q. Tan, Y. Lin, et al., *Anal. Chem.* 90 (2018) 11996–12003.
- [42] Y. Zhuo, D. Zhong, H. Miao, et al., *RSC Adv.* 5 (2015) 32669–32674.